J. Geomag. Geoelectr., **49**, 791–800, 1997

Two-Dimensional Inversion of Oklahoma EMAP Data with Smoothness Regularization

Toshihiro UCHIDA

Geological Survey of Japan, 1-1-3 Higashi, Tsukuba, Ibaraki 305, Japan

(Received February 24, 1995; Revised January 15, 1996; Accepted February 5, 1996)

Two-dimensional inversion has been applied to Electromagnetic Array Profiling (EMAP) data obtained in Oklahoma, USA. Since the data comprise scalar impedances measured along a survey line, a TM-mode inversion was performed on the original data, under the assumption that the survey line is perpendicular to the geologic strike. The inversion method applied is a linearized least-squares scheme with smoothness regularization. The "optimum smoothness" is selected based on a statistical criterion, ABIC (Akaike's Bayesian Information Criterion), which is derived from Bayesian statistics and the entropy-maximization theorem. Starting from a homogeneous earth as an initial guess, the inversion iteratively modifies the model structure until the observations are matched in a statistical sense and parameter modification becomes almost zero. The final two-dimensional models generally show a very conductive host formation (less than 10 Ω·m) with two large resistive bodies of approximately 100 Ω·m embedded near the middle of the survey line.

1. Introduction

Smoothness regularization is commonly applied in geophysical inversion problems. For these tasks, choice of an optimum smoothness is a key factor in obtaining a reliable final model. Constable *et al.* (1987) and deGroot-Hedlin and Constable (1990) introduced a technique to produce the smoothest model for magnetotelluric (MT) inversion which achieves a weighted root-mean-square (rms) misfit of 1. For this method, we have to have a reasonable estimate of observation error prior to the inversion in order to set a tolerable rms misfit. This is not always easy for real field data, and in practice, we set the tolerable final misfit in a subjective manner.

Uchida (1993a) and Uchida and Ogawa (1993) utilized a statistical approach to find a suitable smoothness based on ABIC, a criterion proposed by Akaike (1980), which is based on Bayesian statistics and the maximum entropy theorem. The optimum smoothness sought for each iteration of the inversion is controlled by the trade-off between data misfit and model roughness, and is truly objective in a rigorous statistical sense. The optimum smoothness decided by the ABIC-minimization scheme depends on the observation error. When the data quality is poor, a large smoothing factor (a smoother model) is chosen to compensate for a large misfit. If the observation error is small, a weak smoothness is chosen and the misfit minimization becomes dominant. Information contained in the data is efficiently used to produce a rougher and more realistic model. However, this method usually requires a massive computer facility to deal with real field data because a set of accurate model responses and partial derivatives are necessary to solve the problem with the least-squares scheme.

Inversion methods with some kind of approximation, such as the rapid relaxation inversion (Smith and Booker, 1991) and the approximate inverse mapping (Oldenburg and Ellis, 1991), need a smaller computation time, although they may suffer from some drawbacks of model reliability and stability when data quality is poor.

Uchida (1993b) applied the ABIC-minimization scheme to obtain a two-dimensional (2-D) inversion of a public domain MT dataset, COPROD2, to test the feasibility of the method. In

this paper, the method is applied to the inversion of Electromagnetic Array Profiling (EMAP) data obtained from oil exploration in Oklahoma, USA.

2. Inversion Method

The inversion scheme used here is described in Uchida (1993a). It is based on the linearized least-squares inversion with a smoothness constraint. For this method, we have to minimize a functional U,

$$U = \| Wd - WF(m) \|^2 + \alpha^2 \| Cm \|^2, \tag{1}$$

where W is a weighting matrix, d is observed data, and m is a model. A non-linear function F works on the model m to produce MT responses. α is a smoothing parameter, and C is a roughening matrix. The diagonal matrix, W, is obtained from the observation error of the measured data. The first term on the right-hand side is the data misfit and the second term is the model roughness. Since F is non-linear, we first linearize it about a starting model, then modify the model iteratively to minimize U.

At the k-th iteration, we solve the following equation to obtain the model at the $(k+1)$-th iteration, m_{k+1}.

$$\left\{ (WA)^T (WA) + \alpha^2 C^T C \right\} m_{k+1} = (WA)^T \left(W\hat{d} \right), \tag{2}$$

where A is a Jacobian matrix (sensitivity matrix) consisting of first-order partial derivatives of the responses with respect to the parameters, and

$$\hat{d} = d - F(m_k) + Am_k.$$

The smoothing factor, α, which is used to trade-off between the contributions of the two terms, needs to be carefully selected. The ABIC minimization method is used for this purpose. We define probability density functions (pdf) for the misfit minimization and, simultaneously, the roughness minimization. A Bayesian pdf (or likelihood), $L(d)$, is defined as

$$L(d) = \int p(d|m)\pi(m)\, dm, \tag{3}$$

where $p(d|m)$ is a pdf of the misfit minimization and $\pi(m)$ is a pdf of the roughness minimization. When we assume that the observation error is Gaussian with zero mean and variance σ^2, a pdf of the misfit minimization is given by

$$p(d|m) = \left(\frac{1}{2\pi\sigma^2} \right)^{\frac{N}{2}} \exp\left\{ -\frac{1}{2\sigma^2} \| Wd - WF(m) \|^2 \right\}, \tag{4}$$

where N is the number of observations. Then, we assume that the spatial derivative of resistivity is Gaussian with zero mean and variance-covariance $\sigma^2 \left(\alpha^2 C^T C \right)^{-1}$. A pdf of the roughness minimization is given by

$$\pi(m) = \left(\frac{1}{2\pi\sigma^2} \right)^{\frac{M-1}{2}} \left| \alpha^2 C^T C \right|^{\frac{1}{2}} \exp\left(-\frac{\alpha^2}{2\sigma^2} \| Cm \|^2 \right), \tag{5}$$

where M is the number of the parameters, and $|\cdot|$ denotes the determinant of a matrix. Substituting Eqs. (4) and (5) into Eq. (3), we obtain the Bayesian likelihood.

We now seek a model that maximizes the Bayesian likelihood. This is equivalent to the minimization of U. The optimum smoothness is obtained in the process of the likelihood maximization. For this purpose, a parameter $ABIC$ is defined, following Akaike (1980), as

$$ABIC = (-2)\log(\max L(d)) + 2\dim(\text{hyperparameters}), \tag{6}$$

where "dim" denotes the dimension of the hyperparameters. The smoothing factor, α, is the only hyperparameter in this case. A smaller value of $ABIC$ indicates a larger likelihood, hence a better model. When we run an iterative inversion starting from an initial model, the optimum smoothness is chosen by minimizing $ABIC$ at each iteration. In this work, seven trial smoothing factors were tested at each iteration to determine the minimum $ABIC$, and hence the optimum smoothness.

Calculation of the 2-D model response required for each iteration is accomplished using the finite-element method. Each of several elements are grouped into an individual block, which is assigned a distinct resistivity to be determined. Topography can be incorporated in the finite-element mesh. For the roughening operator, C, either second-order differentiation (2-D Laplacian) or first-order differentiation (1-D) can be applied. The 2-D Laplacian operator is expressed as the following roughening matrix of $M \times M$ elements.

$$\begin{bmatrix} -1 & c_{13} & 0 & c_{14} & & & & 0 \\ c_{22} & -1 & c_{23} & 0 & c_{24} & & & \\ 0 & c_{32} & -1 & c_{33} & 0 & c_{34} & & \\ c_{41} & 0 & c_{42} & -1 & c_{43} & 0 & c_{44} & \\ & & & & \cdot & & & \\ & & & & & \cdot & & \\ & & & & & & \cdot & \\ 0 & & & & c_{M1} & 0 & c_{M2} & -1 \end{bmatrix}, \tag{7}$$

where M is the number of the blocks. The sum of each row of the matrix has to be zero. The 1-D first-order differentiation is given by,

$$\begin{bmatrix} -c_1 & c_1 & & & & & & 0 \\ & -c_2 & c_2 & & & & & \\ & & \cdot & & & & & \\ & & & -c_i & c_i & & & \\ & & & & \cdot & & & \\ & & & & & -c_{M-1} & c_{M-1} & \\ -1 & 0 & 1 & & & & & \\ & -1 & 0 & 1 & & & & \\ & & \cdot & & & & & \\ & & & \cdot & & & & \\ 0 & & & & -1 & 0 & 1 & \end{bmatrix}, \tag{8}$$

where the upper half of the matrix is for the horizontal differentiation, and the lower half corresponds to the vertical differentiation. c_i is given by a ratio between horizontal and vertical sizes of the i-th block. I refer to the second-order differentiation as "*smoothness*" constraint, and the first-order differentiation as "*flatness*" constraint.

Minimum noise (a noise floor) is assumed to be 1%. This means that when the standard deviation of observation error is estimated to be less than 1%, it is assigned a value of 1%. The least-squares inversion is performed with weights calculated as reciprocals of observation errors. The starting model is a homogeneous earth of arbitrary resistivity. The inversion is repeated until convergence is attained. "Convergence" is defined by changes in the rms misfit, model parameters and $ABIC$ as the iteration proceeds.

The inversion is usually well behaved, converging stably. However, on occasion $ABIC$ and/or the rms misfit begin to increase after several iterations. This may be caused by a breakdown of the local linearity assumption for partial derivatives, or a breakdown of the underlying 2-D assumption. In such a case, the inversion step is adjusted using a damping operation, effected by

adding a diagonal matrix to the roughening matrix. The optimum damping can also be chosen based on the ABIC minimization.

3. Data and Inversion

The northeast-southwest trending EMAP line under consideration here is approximately 30 km (Fig. 1). Ninety-three measurement sites are distributed along the line with an interval of about 300 m between stations, except for a large gap at Site 301 where the line crosses a lake. For the EMAP data, an impedance (ρ_{xy}) is calculated from an electric field measurement along the line and the magnetic field perpendicular to it. The general geologic strike is approximately northwest-southeast (Booker, 1994). Therefore, it is reasonable to assume a 2-D structure, with strike perpendicular to the measurement line. The number of measured frequencies is forty, from 0.0005 Hz to 380 Hz.

Surface elements of a finite-element mesh need to be small enough to compute the high-frequency response accurately. However, to model the whole survey line with a single mesh of small elements would require a huge amount of computation time. In this work, therefore, 12 frequencies ranging from 0.0059 Hz to 12 Hz were first picked for the inversion. Data with observation error greater than 200% in apparent resistivity and 32 degrees in phase were omitted. As the long period data were deemed too noisy, the lowest frequency used was 0.0059 Hz. To check the dependency of the inversion on the data density, a 6-frequency subset, from 0.0059 Hz to 6 Hz, was also prepared. The number of observed data used for the inversion, counting apparent resistivity and phase separately, was 2171 for the 12-frequency dataset, and 1077 for the 6-frequency set.

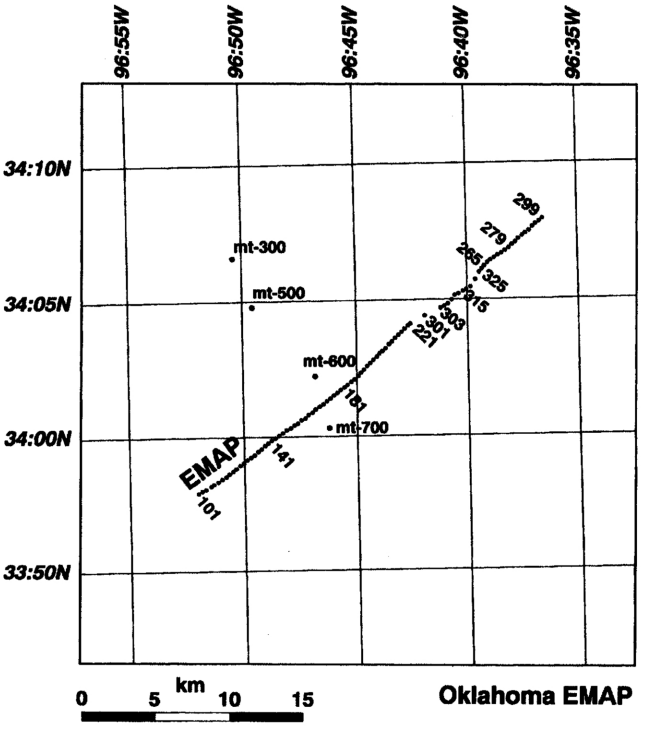

Fig. 1. The Oklahoma EMAP survey line. The frame is defined by UTM coordinates. Four additional magnetotelluric sites are also shown.

The original impedances, not EMAP-filtered, were used for the inversion. Matching between the observations and the model responses was examined in the natural logarithmic domain.

Apparent resistivity and phase pseudosections of the 12-frequency set are shown in Fig. 2. Apparent resistivity is generally very low at all of the sites. Two deep resistive zones are recognizable beneath sites 10 km and 20 km along the line. Phases are consistent with these anomalies.

Finite-element modeling performed for the inversion assumed a TM mode response. The average size of the surface elements was about 300 m horizontally and 25 m vertically. This mesh generates a numerical error of less than 0.5% in apparent resistivity and less than 0.1 degree in phase at all frequencies for a 10 Ω·m half space, which was used as an initial model. Topography was kept flat with an elevation of 100 m. The number of resistivity blocks used was 970 for both datasets.

The inversion behaved very stably and reached convergence for the 6-frequency dataset. However, for the 12-frequency set, a damping operation was required to achieve good convergence. Figure 3 shows how the rms misfit and *ABIC* varied with respect to the smoothing factor α at each iteration for the 6-frequency dataset, and how the parameter modification step decreases as a function of the iteration. The smoothing factor which minimizes *ABIC* is larger than the one which minimizes the rms misfit at later iterations. The parameter modification was negligible after the eighth iteration. The models from the fifth iteration onwards appear to be almost the

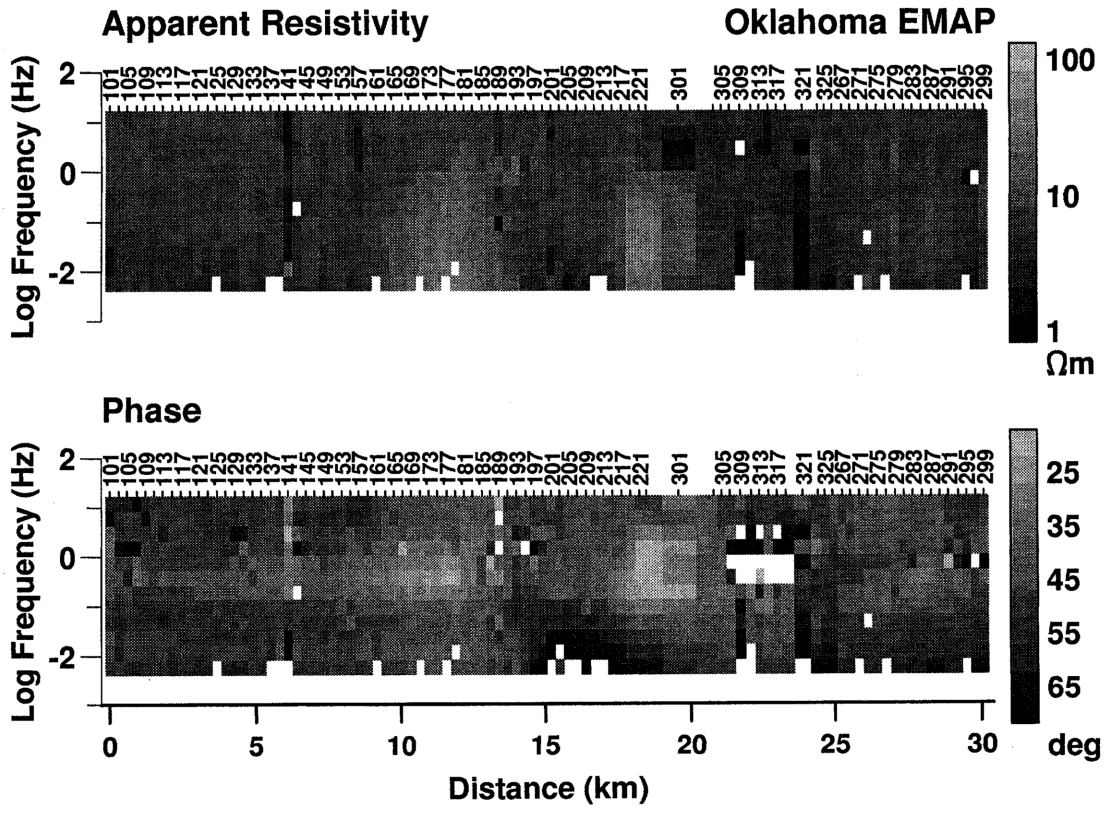

Fig. 2. Apparent resistivity and phase pseudosections of the 12-frequency dataset.

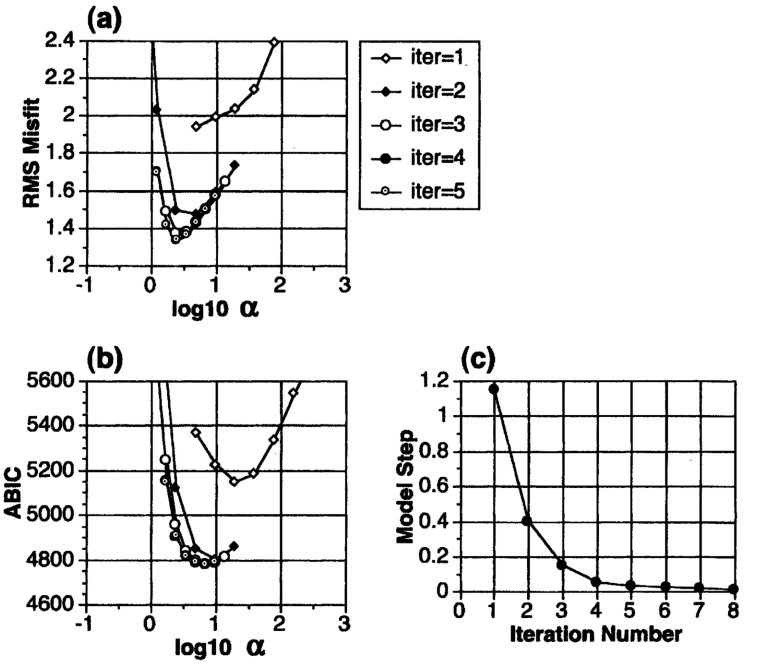

Fig. 3. (a) Weighted rms misfit and (b) *ABIC* as a function of the smoothing factor. (c) The parameter modification step versus iteration number for the 6-frequency inversion with the *smoothness* constraint.

same, as is shown later.

4. Two-Dimensional Models

The utility of the two kinds of constraints, *smoothness* and *flatness*, were tested for the 6-frequency dataset. Only the *smoothness* constraint was applied to the 12-frequency set. The final models for the three cases are shown in Fig. 4. Observed and calculated apparent resistivity and phase curves at every third site are shown in Fig. 5. The average value of final normalized rms misfits was approximately 1.4 assuming a 1% noise floor. This implies that the estimated error bars were reasonably accurate. Visual inspection of Fig. 5 suggests that the fit between observed and calculated values is good. However, there are a number of outliers which can not be explained by the models. Most of these have large observation errors.

The three models (Fig. 4) are very similar. Features common to all three models can be interpreted as true underground structure. The resistivity structures shallower than 5 km are almost the same for the models, except that the 12-frequency model provides more detail. The smoothing factor chosen at the final iteration is smaller for the 12-frequency set.

There are some major horizontal discontinuities recognizable in the apparent resistivity pseudosection which are caused by static shifts (Fig. 2). However, their effects on the inverted 2-D sections are not significant. Resistivities of surficial blocks vary laterally, block by block, although those of deeper blocks vary smoothly in the horizontal direction. It seems that the spatial fluctuation of the TM-mode apparent resistivity due to the static shifts is compensated by the resistivities of the surface blocks, whereas resistivities of deeper blocks are smoothed by the constraint. Thus the practical effect of the smoothing operation is to compensate for static shift in

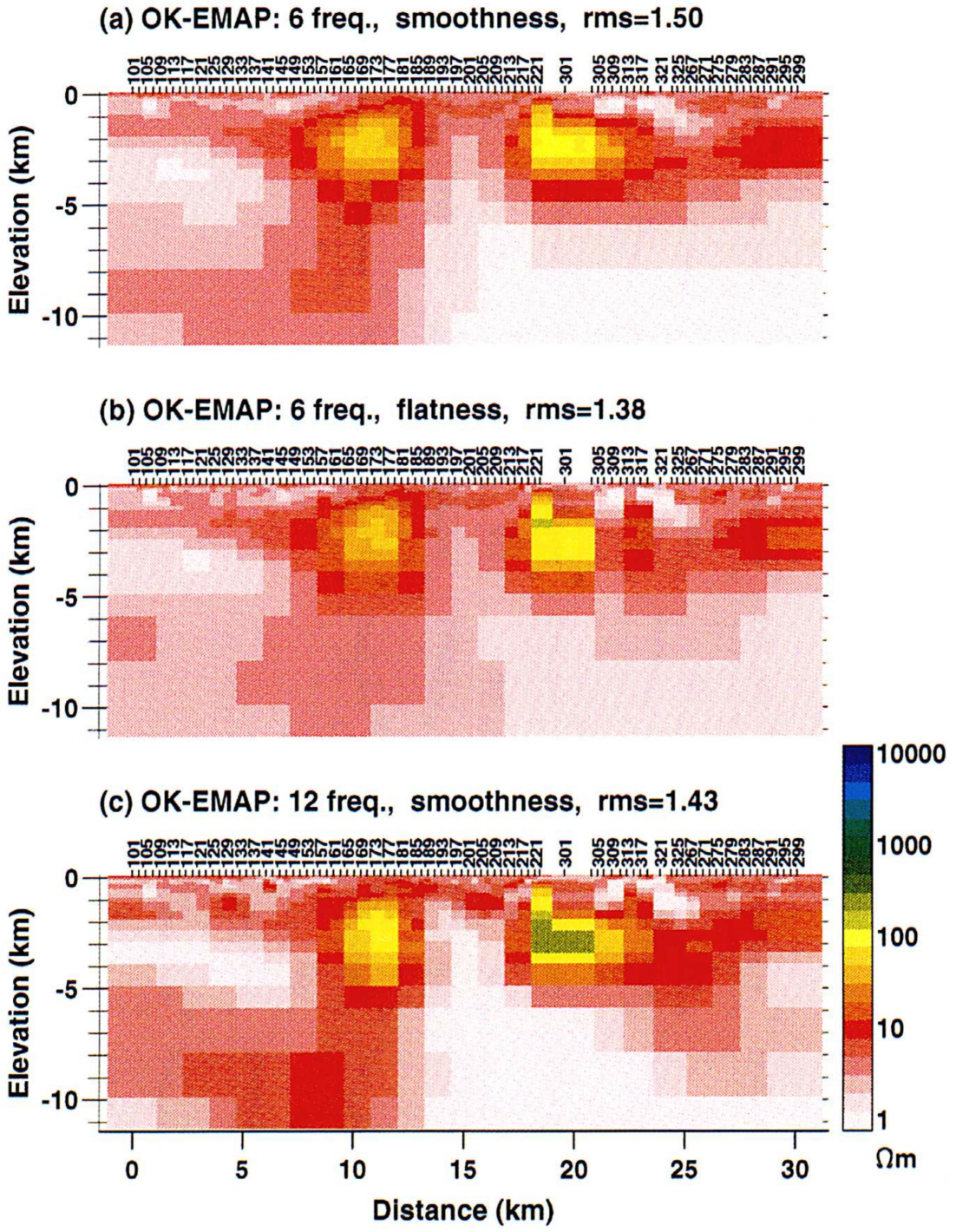

Fig. 4. Inverted resistivity models of the Oklahoma EMAP data. (a) 6 frequencies with *smoothness* constraint, (b) 6 frequencies with *flatness* constraint, and (c) 12 frequencies with *smoothness* constraint.

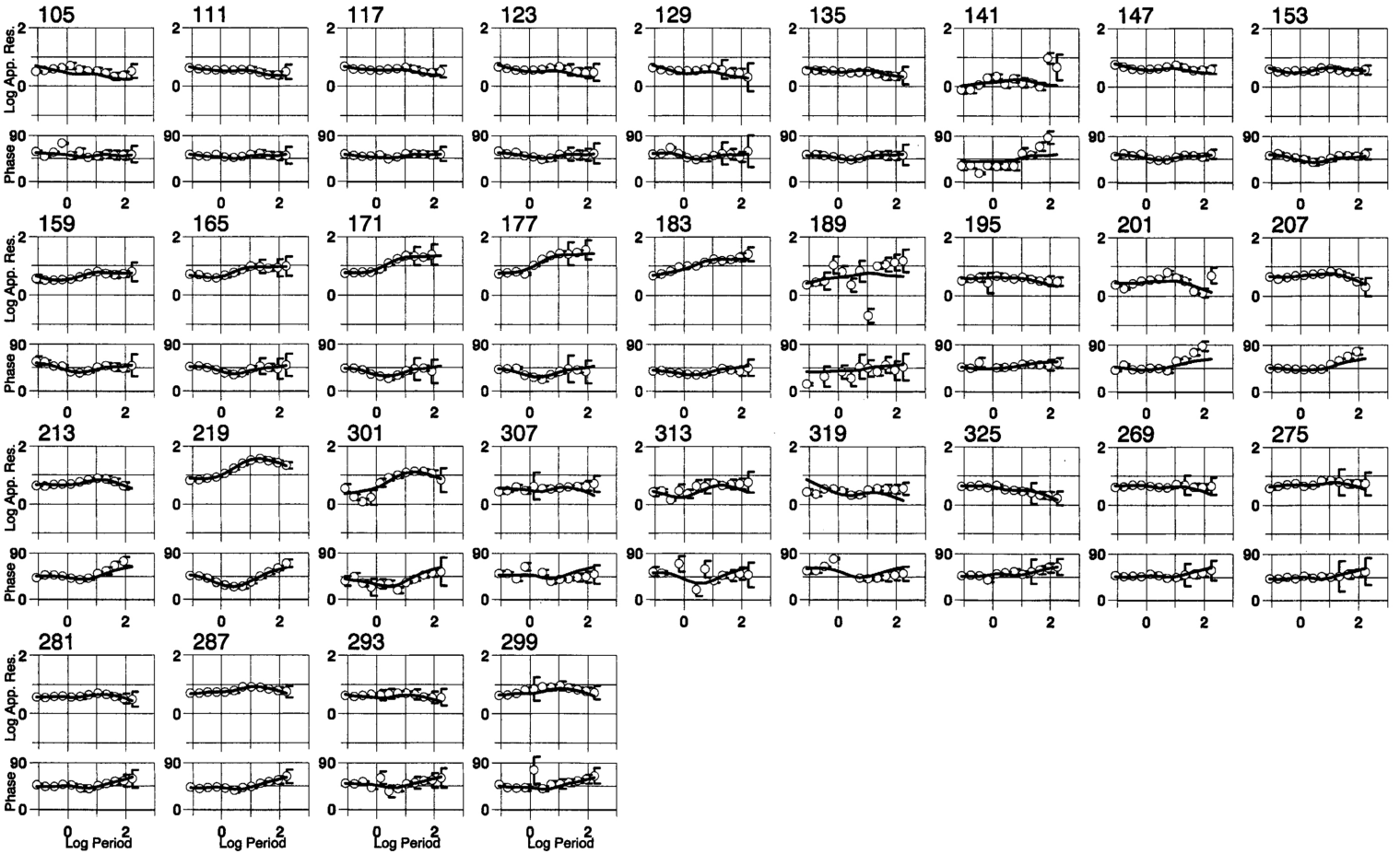

Fig. 5. Observed apparent resistivities and phases (open circles) and those calculated from the model shown in Fig. 4(c) (solid lines) for the 12-frequency TM data. Log10 apparent resistivity (Ω·m) and phase (degrees) versus log10 period (seconds) are shown for every third site. Observation errors of one standard deviation are indicated by vertical bars.

the near surface resistivity rather than producing spurious anomalies at the deeper parts of the model.

The resistivity of the host formation is generally very low, less than 10 Ω·m, across the entire section, with the deeper part of the right-hand side of the section being very conductive. The resistivity of the shallow part is rather high, and there are two large resistive anomalies (approx. 100 Ω·m) at locations 10 km and 20 km along the profile. When we examine the shallow part of the models, up to a depth of 2 km, there are three syncline-like structures whose axes are approximately at sites 141, 201 and 321. The high-resistivity anomalies described above, beneath sites 173 and 301, separate these syncline structures. The detailed geological information of the surveyed area is not public yet. However, the syncline structures seem to be filled with conductive sediments (see Booker (1994) for geological background).

When we compare the *smoothness* and *flatness* constraints for the 6-frequency data, vertical discontinuities are more dominant for the latter. This is due to the form of the roughening matrix for the *flatness* constraint. However, extremely conductive anomalies become more moderate for the *flatness* case; e.g., for the conductive basement in the right of the section. Again we emphasize that the features common to all three models are the significant features (except for the surficial blocks) with differences being mainly due to different forms of the artificially-imposed reguralizations.

5. Conclusions

Three 2-D inversions were performed upon the Oklahoma EMAP data, using different subsets of the data and the form of the roughening operator. The inversions were stable and converged. The final weighted rms misfits were approximately 1.4. This suggests that the estimate of observation error is reasonably accurate.

On comparison of those models, some common features are recognizable, which we can ascribe to real earth structure. The models generally show a very conductive host formation, less than 10 Ω·m, in which two large resistive bodies of approximately 100 Ω·m, are embedded in the middle of the survey line.

Because of the large volume of data and number of unknown parameters, and due to the relatively long survey line, the author was forced to use a CRAY system to obtain the results within a tolerably short turnaround time.

The author is grateful for A. G. Jones of Geological Survey of Canada for providing the Oklahoma EMAP data, and for H. Bibby of the Institute of Geological and Nuclear Sciences Limited, New Zealand, for refining the manuscript. The computation was carried out on the CRAY C916 system at the Computer Center (RIPS), the Agency of Industrial Science and Technology, Tsukuba.

REFERENCES

Akaike, T., Likelihood and Bayes procedure, in *Bayesian statistics*, edited by Bernardo, J. M., M. H. deGroot, D. V. Lindley, and A. F. Smith, pp. 143–166, University Press, Valencia, Spain, 1980.

Booker, J. T., RRI inversion of the Oklahoma EMAP data, Paper presented at *Second Magnetotelluric Data Interpretation Workshop (MT-DIW2)*, held in Cambridge, England, August 5–6, 1994.

Constable, S. C., R. L. Parker, and G. Constable, Occam's inversion: a practical algorithm for generating smooth models from electromagnetic sounding data, *Geophysics*, **52**, 289–300, 1987.

deGroot-Hedlin, C. and S. C. Constable, Occam's inversion to generate smooth, two-dimensional models from magnetotelluric data, *Geophysics*, **55**, 1613–1624, 1990.

Oldenburg, D. W. and R. G. Ellis, Inversion of geophysical data using an approximate inverse mapping, *Geophys. J. Int.*, **105**, 325–353, 1991.

Smith, J. T. and J. R. Booker, Rapid inversion of two- and three-dimensional magnetotelluric data, *J. Geophys. Res.*, **96-B3**, 3905–3922, 1991.

Uchida, T., Smooth 2-D inversion for magnetotelluric data based on statistical criterion ABIC, *J. Geomag. Geoelectr.*, **45**, 841–858, 1993a.

Uchida, T., Inversion of COPROD2 magnetotelluric data by use of ABIC minimization method, *J. Geomag. Geoelectr.*, **45**, 1063–1071, 1993b.

Uchida, T. and Y. Ogawa, Development of Fortran code for two-dimensional magnetotelluric inversion with smoothness constraint, *Geological Survey of Japan Open-File Report*, No. 205, 115 pp., 1993.